AGU PUBLICATIONS

Geophysical Research Letters

RESEARCH LETTER
10.1002/2015GL064048

Key Points:
- Reconstruction of the timing and structure of HS1-related SAMS precipitation
- During HS1 a widespread increase of SAMS rainfall is termed as Mega SACZ
- SAMS responds almost instantaneously to cooling over North Atlantic

Supporting Information:
- Texts S1–S3 and Figures S1–S8, and Table S1

Correspondence to:
N. M. Stríkis,
strikis@gmail.com

Citation:
Stríkis, N. M., et al. (2015), Timing and structure of Mega-SACZ events during Heinrich Stadial 1, *Geophys. Res. Lett.*, *42*, 5477–5484, doi:10.1002/2015GL064048.

Received 28 MAR 2015
Accepted 3 JUN 2015
Accepted article online 6 JUN 2015
Published online 3 JUL 2015

Timing and structure of Mega-SACZ events during Heinrich Stadial 1

Nicolás M. Stríkis[1], Cristiano M. Chiessi[2], Francisco W. Cruz[1], Mathias Vuille[3], Hai Cheng[4], Eline A. de Souza Barreto[1], Gesine Mollenhauer[5,6], Sabine Kasten[5,6], Ivo Karmann[1], R. Lawrence Edwards[4], Juan Pablo Bernal[7], and Hamilton dos Reis Sales[8]

[1]Instituto de Geociências, Universidade de São Paulo, São Paulo, Brazil, [2]Escola de Artes, Ciências e Humanidades, Universidade de São Paulo, São Paulo, Brazil, [3]Department of Atmospheric and Environmental Sciences, University at Albany, Albany, New York, USA, [4]Department of Earth Sciences, University of Minnesota, Twin Cities, Minneapolis, Minnesota, USA, [5]MARUM-Center for Marine Environmental Sciences, University of Bremen, Bremen, Germany, [6]Alfred Wegener Institute for Polar and Marine Research, Bremerhaven, Germany, [7]Centro de Geociencias, Universidad Nacional Autonoma de Mexico, Querétaro, Mexico, [8]Instituto Federal de Educação, Ciência e Tecnologia do Norte de Minas Gerais-IFET, Januária, Brazil

Abstract A substantial strengthening of the South American monsoon system (SAMS) during Heinrich Stadials (HS) points toward decreased cross-equatorial heat transport as the main driver of monsoonal hydroclimate variability at millennial time scales. In order to better constrain the exact timing and internal structure of HS1 over tropical South America, we assessed two precisely dated speleothem records from central-eastern and northeastern Brazil in combination with two marine records of terrestrial organic and inorganic matter input into the western equatorial Atlantic. During HS1, we recognize at least two events of widespread intensification of the SAMS across the entire region influenced by the South Atlantic Convergence Zone (SACZ) at 16.11–14.69 kyr B.P. and 18.1–16.66 kyr B.P. (labeled as HS1a and HS1c, respectively), separated by a dry excursion from 16.66 to 16.11 kyr B.P. (HS1b). In view of the spatial structure of precipitation anomalies, the widespread increase of monsoon precipitation over the SACZ domain was termed "Mega-SACZ."

1. Introduction

Heinrich Stadials (HS) are important components of millennial-scale climate variability, occurring during specific stadial phases as massive depositional episodes of ice-rafted debris in the North Atlantic [*Heinrich*, 1988; *Hemming*, 2004; *Sánchez-Goñi and Harrison*, 2010]. Global-scale variations in the hydrologic balance have been well documented during HS, in particular the antiphased response in the summer monsoon regimes of both hemispheres [*Broecker et al.*, 2009; *Cheng et al.*, 2012; *Chiessi et al.*, 2009; *Cruz et al.*, 2005; *Dupont et al.*, 2010; *Wang et al.*, 2004]. The antiphased tropical precipitation response results from an adjustment in the location of the Intertropical Convergence Zone (ITCZ) to cooling in extratropical areas of the Northern Hemisphere and consequent changes in the interhemispheric sea surface temperature (SST) gradient [*Chiang and Bitz*, 2005; *Cvijanovic and Chiang*, 2013].

Paleoclimate reconstructions from tropical and subtropical areas have ascribed two distinct hydrologic periods to HS1, which give the event a twofold structure [*Broecker et al.*, 2009; *Escobar et al.*, 2012; *Dupont et al.*, 2010; *Zhang et al.*, 2014]. However, some climate fluctuations observed in tropical climate at the time of HS1 are not fully understood. For instance, a transition between two distinct events labeled as Big Dry (17.5–16.1 kyr B.P.) and Big Wet (16.1–14.6 kyr B.P.) recorded in lake sediments over western North America [*Broecker et al.*, 2009; *Allen and Anderson*, 2000] occurs concomitantly with an abrupt weakening of the East Asian monsoon at 16.1 kyr B.P. [*Wang et al.*, 2001; *Zhang et al.*, 2014]. Furthermore, over the Central American and African monsoon domains [*Escobar et al.*, 2012; *Stager et al.*, 2011] paleoprecipitation reconstructions suggest a double-plunge structure during HS1, with severe droughts peaking at ~17 and 16 kyr B.P.. Yet despite the increased number of studies that report abrupt changes in summer monsoon regimes in both hemispheres [*Cheng et al.*, 2012; *Chiessi et al.*, 2009; *Dupont et al.*, 2010], the timing and structure of HS1 over the South American Monsoon System (SAMS) domain are still poorly documented. Understanding the exact timing of climate anomalies during HS1 in the tropics is, however, a necessity to assess if climatic perturbations reported from different monsoon domains represent synchronous

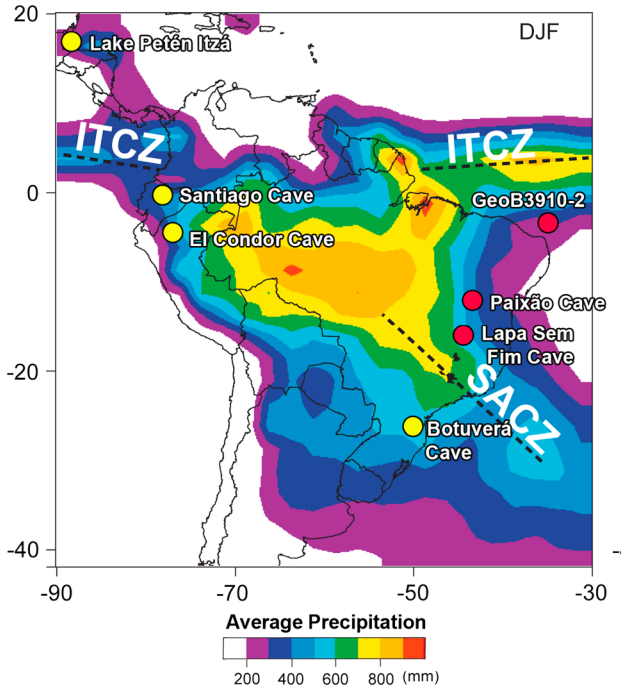

Figure 1. Schematic diagram showing long-term mean (1979–2000) austral summer (December-January-February) precipitation in South America from the Climate Prediction Center Merged Analysis of Precipitation. Dashed lines indicate the main climatological features of the South American Monsoon System: South Atlantic Convergence Zone (SACZ), and Intertropical Convergence Zone (ITCZ). Red dots indicate our study sites, and yellow dots refer to other paleoclimate records discussed in this paper.

manifestations of the same global-scale event, different events, or even one time-transgressive event [e.g., *Alley and Ágústsdóttir*, 2005].

Unlike most other monsoon systems, SAMS precipitation is largely concentrated in tropical areas, with the South Atlantic Convergence Zone (SACZ) (Figure 1) as an important monsoon component, protruding as a lower tropospheric convective belt from the western Amazon to southeastern Brazil and the South Atlantic [*Gandu and Silva Dias*, 1998; *Chen and Weng*, 1999; *Carvalho et al.*, 2004; *Vera et al.*, 2006; *Marengo et al.*, 2012]. Despite the great relevance of the SACZ as the main zone of monsoonal moisture convergence and interactions with midlatitude wave trains, the impact of HS on the strength and position of the SACZ is poorly understood. Here we present a multiproxy paleoprecipitation reconstruction during HS1 covering areas affected by both the SACZ and the ITCZ. Our paleomonsoon archives comprise well-dated speleothem records from central-eastern and northeastern Brazil, where the precipitation is exclusively due to SACZ activity. We compare these speleothem records with terrestrial organic and inorganic matter input into the western equatorial Atlantic, which reflects continental precipitation directly affected by the ITCZ. When combined, these new paleoclimate records provide unique insights into the timing and hydrologic expression of HS1 over tropical South America.

2. Site Descriptions

2.1. Speleothem Records

The speleothems used in this study were collected from two distinct caves located in central-eastern Brazil, namely Lapa Sem Fim Cave (16°08′52″S, 44°36′38″W) and Paixão Cave at the southern border of northeastern Brazil (12°37′5.61″S, 41°1′.35″W). The distance between the two caves is about 460 km (Figure 1).

The Lapa Sem Fim Cave is located close to the NW-SE axis of the SACZ. Annual mean precipitation at Lapa Sem Fim Cave is around 930 mm based on meteorological data from 1975 to 2009 recorded at stations located 20 km from the cave entrance. At Paixão Cave, the annual mean precipitation is around 640 mm, based on an 11 year record between 1964 and 1975 from meteorological stations located 18 km to the west of the cave entrance (source: www2.ana.gov.br).

At both sites precipitation occurs almost exclusively during the active period of the SAMS (~95% of the total annual precipitation), starting in October and ending in April, with maximum activity between November and February that corresponds to almost 70% of total annual precipitation (Figure 1). In tropical areas, deep convection and vertical uplift of air masses produce an isotopic effect known as "amount effect" [*Bony et al.*, 2008; *Risi et al.*, 2008; *Rozanski et al.*, 1993; *Vuille et al.*, 2003; *Vuille and Werner*, 2005]. In essence, the amount effect is the inverse proportional variation of the $\delta^{18}O$ of the rainfall with the amount of precipitation [*Bony et al.*, 2008; *Risi et al.*, 2008; *Rozanski et al.*, 1993]. A local isotopic monitoring program of rainfall performed since 2011 shows that the isotopic composition of rainfall is strongly controlled by

the amount effect, presenting a strong negative correlation ($R^2 = 0.73$) between monthly rainfall amount and monthly weighted mean $\delta^{18}O$ (Figure S1 in the supporting information). The correlation is consistent with data from the International Atomic Energy Agency-Global Network of Isotopes in Precipitation observed at Brasília, where correlation was equally high during the period from 1963 to 1987 ($R^2 = 0.68$) and where precipitation is climatologically identical to our study area (Figure S1).

2.2. Marine Records

The marine records reported here are based on marine sediment core GeoB3910-2 collected ~ 120 km off the coast of northeastern Brazil (4°14′42.00″S, 36°20′42.00″W; 2362 m water depth) [*Fischer et al.*, 1996].

Meridional ITCZ migrations control precipitation in the catchment area of the rather small drainage basin (i.e., Piranha River) that provides continental sediments to our core site [*Jaeschke et al.*, 2007]. Apart from a narrow coastal strip where annual mean precipitation is higher than 1250 mm, the interior of northern Northeastern Brazil is semiarid with annual precipitation of 300–900 mm based on monitored time series from 1910 to 1985 (source: www2.ana.gov.br). In this region, 80% of the annual rainfall occurs between February and May [*Hastenrath*, 1990; *Rao et al.*, 1996] (more details in the supporting information Text S1).

3. Methods

3.1. Speleothem Records: Oxygen Isotope and Geochronological Data

Stable oxygen isotope analyses were performed at the Stable Isotope Laboratory at the University of São Paulo. Oxygen isotope ratios are expressed in δ notation, the per mil deviation from the Vienna Peedee belemnite (V-PDB) standard according to the following equation: $\delta^{18}O = [((^{18}O/^{16}O)_{sample}/(^{18}O/^{16}O)_{V\text{-}PDB}) - 1] \times 1000$. The calcite powder was analyzed with an online, automated carbonate preparation system linked to a Finnigan Delta Plus Advantage mass spectrometer. Ages were obtained by using a multicollector inductively coupled plasma mass spectrometry technique (Thermo-Finnigan NEPTUNE) at the University of Minnesota following the procedures described by *Cheng et al.* [2013a]. The B.P. notation refers to the age before present, taking the present as 2000 A.D.

The isotope records of LSF16 and LSF3 were combined in order to produce a single curve for the time period between 19.35 and 14.42 kyr B.P. from Lapa Sem Fim (Figure S2). The Paixão Cave speleothem record is also a combination of two speleothems: PX7 (from 19.19 to 15.03 kyr B.P.) and PX5 (from 14.87 to 12.0 kyr B.P.) (Figure S3; more details in the supporting information Text S2).

3.2. Marine Records: Biomarkers, Geochemistry, and Geochronological Data

To reconstruct the ITCZ activity over northeastern Brazil, we performed Ti/Ca and branched and isoprenoid tetraether (BIT) index measurements on marine sediment core GeoB3910-2. The Ti/Ca ratio in continental margins not affected by major changes in primary productivity and carbonate dissolution [*Arz et al.*, 1998; *Jaeschke et al.*, 2007] can be used as an indicator of the input of continental sediments to the core site [*Govin et al.*, 2012]. Concentrations of Ti and Ca in marine core GeoB3910-2 were determined by inductively coupled plasma optical emission spectrometry after microwave acid total digestion of dried and ground sediments as described, e.g., by *Fischer et al.* [2013].

The BIT index on the other hand reflects the input of soil-derived organic matter to the core site [*Hopmans et al.*, 2004]. The BIT index uses the relative abundance of membrane lipids derived from anaerobic bacteria thriving in soils and peat, compared with crenarchaeol, a structurally related isoprenoid molecule characteristic of ubiquitous marine planktonic and lacustrine thaumarchaeota [e.g., *Schouten et al.*, 2013]. The analytical procedure followed *Hopmans et al.* [2004] (more details in the supporting information Text S2). Both proxies allow the reconstruction of terrestrial organic (i.e., BIT index) and inorganic (i.e., Ti/Ca) fluvial input to the ocean reflecting variations in continental precipitation, in our case strongly controlled by the ITCZ.

The chronological control of the GeoB3910-2 is the same as in *Jaeschke et al.* [2007]. During the period of HS1, from 19 to 14 kyr B.P., the marine core features four ^{14}C ages with dating errors varying from 110 to 70 years. Sedimentation rates at HS1 range between 7 and 23 cm/kyr.

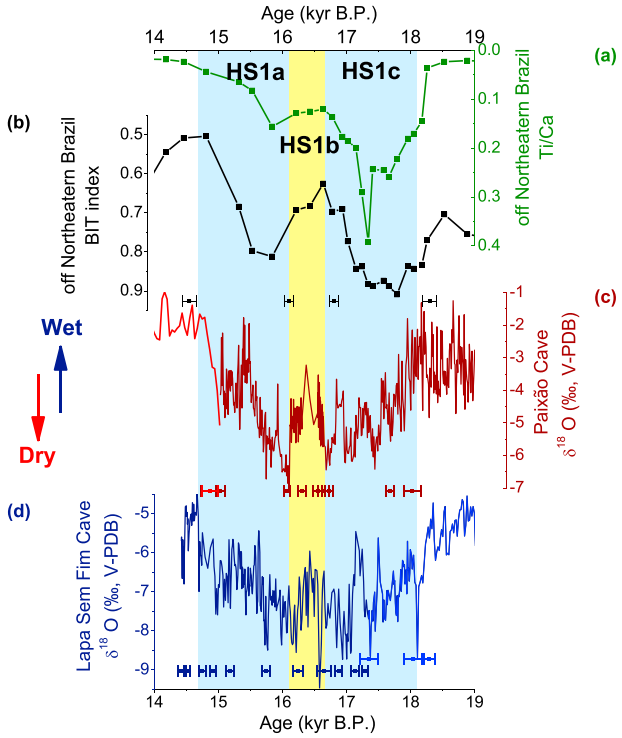

Figure 2. High-resolution South American monsoon system precipitation reconstruction across HS1: (a) Ti/Ca, and (b) Branched and isoprenoid tetraether (BIT) index from marine sediment core GeoB3910-2 raised off northeastern Brazil (this study); (c) composite $\delta^{18}O$ from PX5 (light red) and PX7 (dark red) speleothems collected from Paixão Cave, northeastern Brazil (this study); (d) composite $\delta^{18}O$ from LSF16 (dark blue) and LSF3 (light blue) speleothems collected from Lapa Sem Fim Cave, central-eastern Brazil (this study). Blue and red symbols show U/Th age of speleothems. Black symbols show ^{14}C ages of the marine core. Light blue and yellow vertical shading delimits the intervals of HS1a, HS1b, and HS1c.

4. Results

4.1. Speleothem $\delta^{18}O$ Profiles

A major contribution of this work is the robust chronological control of our speleothem records. The age model of the Lapa Sem Fim Cave record is based on 16 U/Th ages with errors (2σ) < 1%. In total, 12 dates were established for LSF16 covering the period between 14.42 and 18.22 kyr B.P., and 4 dates for LSF3 covering the period between 17.35 and 19.35 kyr B.P. (Table S1). The same applies to the Paixão Cave stalagmites whose age model is based on 11 U/Th dates: two dates for PX5 (ranging from 12.00 to 14.87 kyr B.P.) and nine dates for PX7 (ranging from 15.03 to 19.19 kyr B.P.).

Speleothem $\delta^{18}O$ records from Lapa Sem Fim and Paixão caves are based on 381 and 403 samples, yielding a mean temporal resolution of 12 and 10 years, respectively. The isotope profiles from both cave stalagmites are strikingly similar, both in terms of timing and relative amplitude (more details in the supporting information Text S3). The $\delta^{18}O$ records are characterized by a double-plunge structure during the period corresponding to HS1, which characterizes two phases of increased monsoonal precipitation: the first from 16.11 to 14.69 kyr B.P. and the second from 18.1 to 16.66 kyr B.P., hereafter named HS1a and HS1c, respectively (Figure 2). The two wet events are interrupted by a long-standing dry excursion ranging from 16.66 to 16.11 kyr B.P., hereafter named HS1b (Figure 2).

As a whole, the expression of HS1 over central-eastern Brazil lasts around 3.4 kyr, from 18.1 to 14.69 kyr B.P. The first increase in monsoon precipitation lasted about 1 kyr reaching its maximum between ~17.08 and 16.69 kyr B.P. Over the course of HS1c, both speleothem records describe consistent variations of $\delta^{18}O$ at centennial time scales, characterized by abrupt transitions between wet and dry events (Figure 2). In the speleothem records, the second maximum in monsoon activity (HS1a) starts as an abrupt resumption toward wet conditions at 16.1 kyr B.P. HS1a is characterized by a gradual demise in monsoon precipitation lasting around 1.46 kyr and can be split into two steps separated from each other by a plateau between ~15.6 and ~14.9 kyr B.P., and a more abrupt shift at 14.69 kyr B.P. (Figure 2). The wettest period during HS1a occurs between 16.1 and 15.7 kyr B.P.

4.2. Sedimentary BIT Index and Ti/Ca Profiles

In the investigated marine core, the average sampling resolution is approximately 250 years, varying from 500 to 70 years. Due to the lower sampling resolution, minor internal climate oscillations observed in the speleothems, such as the centennial-scale climate variability described within HS1c, cannot be detected. However, important information about the structure and expression of HS1 over the ITCZ region can still be extracted from the marine records, such as the onset and end of HS1 (Figure 2). The onset of HS1 occurs at 18.2 kyr B.P. and is characterized by a marked increase in the Ti/Ca ratio and BIT index during HS1c. The demise of HS1a over the ITCZ region is characterized by a gradual transition toward drier conditions lasting 1 kyr (from 15.5 until 14.5 kyr) (Figure 2).

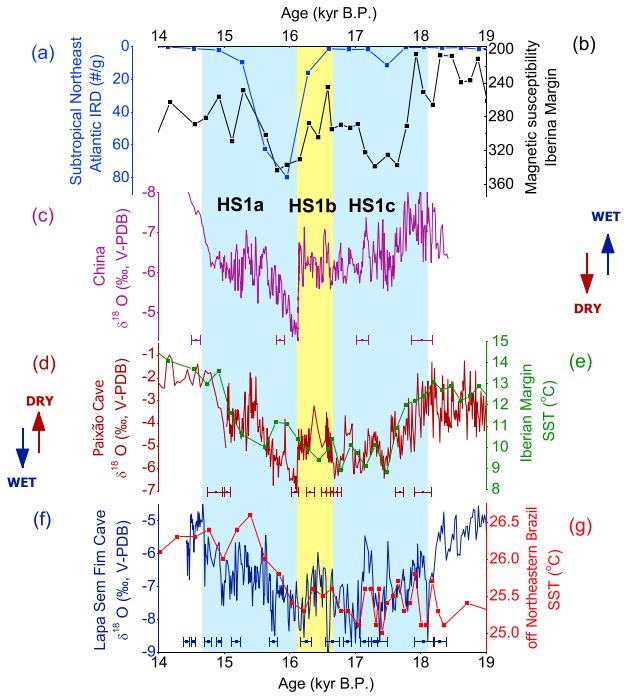

Figure 3. Records of changes in oceanic circulation and continental precipitation across both hemispheres: (a) Ice-rafted debris (IRD) record of marine sediment core SU8118 from the Iberian margin [*Bard et al.*, 2000]; (b) magnetic susceptibility of marine sediment core SU8118 from the Iberian margin [*Thouveny et al.*, 2000]; (c) composite $\delta^{18}O$ of speleothems from Hulu cave, eastern China [*Zhang et al.*, 2014; *Wang et al.*, 2001]; (d) $\delta^{18}O$ of speleothems from Paixão Cave, northeastern Brazil (this study); (e) alkenone sea surface temperature (SST) of marine sediment core SU8118 from the Iberian margin [*Bard et al.*, 2000]; (f) $\delta^{18}O$ of speleothems from Lapa Sem Fim Cave, central-eastern Brazil (this study); and (g) alkenone SST reconstruction of marine sediment core GeoB3910-2, off northeastern Brazil [*Jaeschke et al.*, 2007]. Note the reversed *y* axis in Figures 3a–3c. Light blue and yellow vertical bars delimit the intervals of HS1a, HS1b, and HS1c.

In the marine records, the internal structure of HS1 is also defined by a double plunge with two wet events centered near 17.4 (HS1c) and 15.7 (HS1a) kyr B.P., separated by a distinctly drier excursion (HS1b), similar to the speleothem records. Similarly, the structure of the longest dry event in the marine records, characterized by lower Ti/Ca and BIT index values, is consistent with the variations in $\delta^{18}O$ seen in the speleothems (Figure 2). Overall, the timing of the wet events HS1a (16.11 to 14.69 kyr B.P.) and HS1c (18.1 to 16.66 kyr B.P.) and the drier intervening phase HS1b (16.66 to 16.11 kyr B.P.) is consistent between the speleothem and marine records and reinforces the notion of synchronous changes in climate over a significant portion of the eastern SAMS domain that extends at least from 16°S to 4°S.

5. Discussion

Ranging from 16°S to 4°S our paleomonsoon precipitation records show a consistent scenario of noticeable strengthening of monsoon precipitation over the eastern portion of the SAMS domain embracing areas from central- to northeastern Brazil during HS1 (Figure 2). Equivalent episodes of increasing SAMS precipitation are also reported from the western Amazon basin in speleothem records from El Condor [*Cheng et al.*, 2013b] and Santiago cave [*Mosblech et al.*, 2012], and from southeastern South America, in the Botuverá cave record [*Cruz et al.*, 2005]. Taken together, these records reveal a widespread and pervasive strengthening of monsoonal circulation over South America during HS1 (Figure S5). Here we coin the term "Mega-SACZ" to define episodes of widespread intensification across the entire region influenced by the SACZ as observed during the HS1a and HS1c. The fact that the anomalous increase in monsoon precipitation along the eastern border of the SACZ domain reached 4°S suggests that convective activity related to both the SACZ and the ITCZ contributed to enhanced precipitation in this domain during HS1a and HS1c. The strengthening of the SACZ observed during HS1, the Mega-SACZ episode, is strongly modulated by the cooling of tropical/subtropical areas of the North Atlantic and consequent change in tropical interhemispheric SST gradients. As shown in Figure 3, the strengthening of the SAMS that characterizes the onset of HS1 over the eastern border of the SAMS domain occurs concomitantly with the cooling recorded in the subtropical North Atlantic [*Bard et al.*, 2000]. A similar synchronicity is also present during the demise of the positive monsoon precipitation anomaly of HS1a, when a weakening in the SACZ activity occurs in conjunction with a warming of approximately 4.5°C and 1°C at the Iberian margin [*Bard et al.*, 2000] and off northeastern Brazil [*Jaeschke et al.*, 2007], respectively (Figure 3). In addition, precipitation fluctuations at centennial time scales at the studied sites are consistent with changes in the SST record from GeoB3910-2 [*Jaeschke et al.*, 2007] (Figure 3). Thus, the excellent coupling between our paleomonsoon reconstruction and tropical and extratropical Atlantic SST during HS1 (Figure 3) strongly suggests an almost immediate response of SAMS circulation to changes in cross-equatorial heat transport.

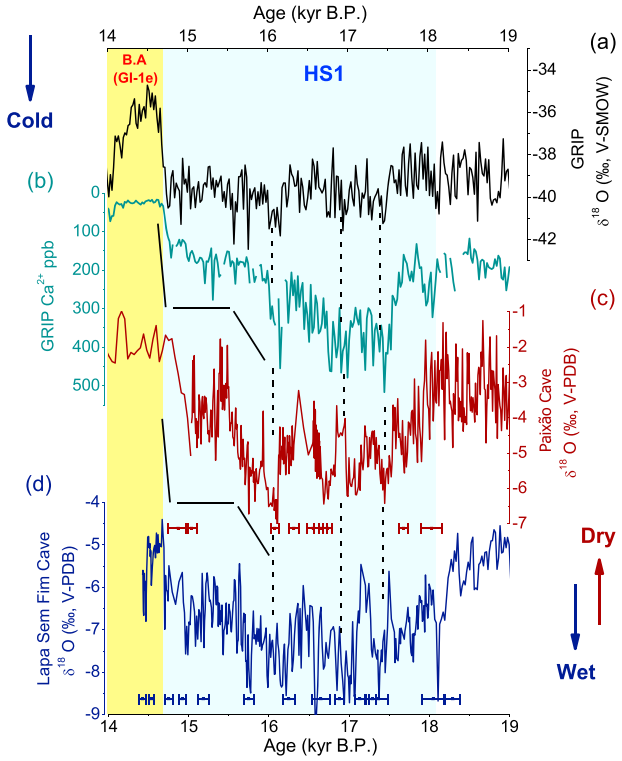

Figure 4. Comparison between (a) $\delta^{18}O$ record from Greenland Ice Core Project (GRIP) ice core plotted versus the Greenland Ice Core Chronology 2005 (GICC05) [*Rasmussen et al.*, 2006]; (b) GRIP Ca^{2+} concentration plotted versus the (GICC05) [*Rasmussen et al.*, 2006]; (c and d) $\delta^{18}O$ from speleothems collected in northeastern and central-eastern Brazil, respectively (this study). Dashed vertical lines connect centennial-scale departures. Light blue and yellow fields delimit the intervals of HS1 and the Bølling-Allerød or Greenland Interstadial (GI) 1e, respectively.

Important features of the Mega-SACZ episodes observed during HS1a and HS1c correspond with noticeable changes in the hydrologic regime of the global tropics but identified and accurately dated for the first time in South America. The double-plunge structure observed in our paleomonsoon precipitation reconstruction mirrors variations in precipitation recorded over lowland Central America described as "symmetric" antiphased pattern between the SAMS and the Central America monsoon regime [*Escobar et al.*, 2012] (Figure S6). The dry excursion presented in our records (i.e., HS1b) was also documented by *Dupont et al.* [2010] based on $\delta^{13}C_{org}$ in sediments from the same marine core investigated in this study (Figure S6).

The weakening of SAMS activity during HS1b is also coherent with a warming in the subtropical North Atlantic (Figure S7). As shown in Figure S7, HS1 SST reconstructions from the subtropical northeastern North Atlantic [e.g., *Pailler and Bard*, 2002 and *Martrat et al.*, 2014] report a similar double-plunge structure with the intervening warm excursion as large as 3°C. The good temporal and structural correspondence between the convective activity over the SACZ region and SST anomalies in the subtropical North Atlantic suggests that a strengthening in the cross-equatorial heat transport, probably driven by intensification in the Atlantic Meridional Overturning Circulation (AMOC), was the possible cause for the drier HS1b.

In order to investigate the dominant multidecadal and centennial modes of climate variability present in our $\delta^{18}O$ time series, we performed wavelet analyses in the isotopic records from Lapa Sem Fim and Paixão caves. As shown in Figure S8, a persistent periodicity with pacing near 64 years was identified in the Lapa Sem Fim isotopic record extending from 17.5 to 15.1 kyr B.P. A similar pacing (persistent between 16 and 15.1 kyr B.P.) was also observed in a record of La Plata River drainage basin discharge [*Chiessi et al.*, 2009] and associated with variability in the SACZ and the AMOC. Our results highlight the pervasive character of the multidecadal variability in the SACZ activity.

Among the main climate fluctuations observed during HS1, the abrupt strengthening in SAMS at 16.1 kyr B.P. (onset of HS1a) presents a remarkable match in the timing and structure with a dramatic weakening of the East Asian monsoon recorded in speleothems from eastern China [*Zhang et al.*, 2014]. The abrupt event at 16.1 kyr B.P. also coincides with the strongest peak of ice-rafted debris (IRD) deposition over the Ruddiman belt during HS1 and with a strengthening of the Northern Hemisphere polar vortex (Figures 3 and 4). Centennial-scale increases in SAMS strength over central-eastern and northeastern Brazil during HS1c, including the abrupt resumption of wet conditions at 16 kyr B.P., closely match the peaks of Ca^{2+} concentration recorded in Greenland ice cores (Figure 4) [*Rasmussen et al.*, 2006]. Thus, in light of the enormous amount of ice discharge necessary to form an IRD layer [*Bond et al.*, 1999; *Hemming*, 2004], we suggest that the abrupt bidirectional change in Northern and Southern Hemisphere monsoons, observed at 16.1 kyr B.P., occurred as a consequence of the adjustment of the ITCZ to Northern Hemisphere

midlatitude cooling caused by the massive surging of icebergs. As clearly documented in the speleothem $\delta^{18}O$ profile, the southward shift of the ITCZ and the strengthening in the SAMS occurred almost instantaneously.

Also noteworthy is the two-step character of the drying trend observed during the demise of HS1a, transitioning rather abruptly from very wet conditions at the onset of HS1 to much drier conditions at the time of Bølling-Allerød. This two-step transition is also very well defined in the reconstruction of the strength of the polar vortex (Figure 4) [*Rasmussen et al.*, 2006]. A more gradual transition is apparent in marine records off northeastern Brazil related to $\delta^{13}C$ of terrigenous organic matter input [*Dupont et al.*, 2010], as well as to SST reconstructions [*Jaeschke et al.*, 2007] (Figures S6 and 3). In both the SAMS and the East Asian monsoon domain [*Zhang et al.*, 2014], the final transition is characterized by an abrupt change at 14.7 kyr B.P. The timing for the onset of the climate anomalies related to the Bølling-Allerød over the SAMS is identical, within dating errors, to the corresponding transition from Greenland Stadial 2.1a to Greenland Interstadial 1e at 14.692 kyr B.P. reported by *Rasmussen et al.* [2014] based on the synchronized Greenland ice core records using the annual layer counted Greenland Ice Core Chronology 2005 (GICC05) (Figure 4).

6. Conclusions

Our multiproxy paleoprecipitation records comprise accurately dated speleothem $\delta^{18}O$-derived variations of monsoon precipitation over central and northeastern Brazil during HS1, which are consistent with organic and inorganic terrestrial input to the western equatorial Atlantic. Our reconstruction of the timing and structure of HS1-related precipitation changes over tropical South America is unprecedented both in terms of its high temporal resolution and dating accuracy. Furthermore, the reported monsoon variations during HS1 are in agreement with changes in Atlantic SST suggesting a rapid reorganization of atmospheric circulation in response to variations in ocean heat transport.

Over the eastern portions of the SAMS domain the footprint of HS1 is characterized by a strengthening of monsoonal circulation involving an intensification of the SACZ and a southward shift of the ITCZ. This pattern is accompanied by enhanced moisture convergence and convection over the western Amazon basin. Our paleoclimate reconstruction supports the notion that the strength and position of the SACZ is sensitive to tropical interhemispheric SST gradients. Finally, our high-resolution and very precisely and accurately dated speleothem records suggest that within dating uncertainty, the response of the SAMS to this Northern Hemisphere forcing during HS1 was synchronous, hence no time lag was required for the SAMS reorganization, following the abrupt cooling over midlatitude areas of the North Atlantic.

Acknowledgments

We thank L. Mancine and O. Antunes for their support during the stable isotope data acquisition at the University of São Paulo. H. Grotheer is acknowledged for organic geochemical analyses determining the BIT index. We are grateful to Pedro L. Silva Dias for fruitful discussions and two reviewers for their helpful comments. We thank the IBAMA and ICMBio for permission to collect stalagmite samples. Marine sediment sample material has been provided by the GeoB Core Repository at the MARUM-Center for Marine Environmental Sciences, University of Bremen, Germany. This work was supported by the Fundação de Amparo à Pesquisa do Estado de São Paulo (FAPESP), Brazil (PhD fellowship to Stríkis) 2011/12087-4; grants to Chiessi 2012/17517-3; Cruz, 2012/50260-6, Karman 2012/01187-4, BIOTA, 2013/50297 by the NSF 1103403 to R.L.E and H.C. and 1303828 to M.V. and DEB 1343578 and NASA through the Dimensions of Biodiversity Program. The data presented in this paper can be found at PANGEA database (http://doi.pangaea.de/10.1594/PANGAEA.847283).

The Editor thanks two anonymous reviewers for their assistance in evaluating this paper.

References

Allen, B. D., and R. Y. Anderson (2000), A continuous, high-resolution record of late Pleistocene climate variability from the Estancia basin, New Mexico, *Geol. Soc. Am. Bull.*, *112*, 1444–1458, doi:10.1130/0016-7606(2000)112<1444:ACHRRO>2.0.CO.

Alley, R. B., and A. M. Ágústsdóttir (2005), The 8 k event: Cause and consequences of a major Holocene abrupt climate change, *Quat. Sci. Rev.*, *24*, 1123–1149, doi:10.1016/j.quascirev.2004.12.004.

Arz, H. W., J. Pätzold, and G. Wefer (1998), Correlated millennial-scale changes in surface hydrography and terrigenous sediment yield inferred from last glacial marine deposits off northeastern Brazil, *Quat. Int.*, *50*(2), 157–166, doi:10.1006/qres.1998.1992.

Bard, E., F. Rostek, J. L. Turon, and S. Gendreau (2000), Hydrological impact of Heinrich events in subtropical South Atlantic, *Science*, *289*(25), 1321–1324, doi:10.1126/science.289.5483.1321.

Bond, G. C., W. Showers, M. Elliot, M. Evans, R. Lotti, I. Hajdas, G. Bonani, and S. Johnsen (1999), The North Atlantic's 1–2 kyr climate rhythm: Relation to Heinrich events, Dansgaard/Oeschger cycles and the Little Ice Age, in *Mechanisms of Global Climate Change at Millennial Time Scales*, *Geophys. Monogr. Ser.*, vol. 112, edited by P. U. Clark, R. S. Webb, and L. D. Keigwin, pp. 35–68, AGU, Washington, D. C.

Bony, S., C. Risi, and F. Vimeux (2008), Influence of convective processes on the isotopic composition ($\delta^{18}O$ and δD) of precipitation and water vapor in the tropics: 1. Radiative–convective equilibrium and Tropical Ocean–Global Atmosphere–Coupled Ocean–Atmosphere Response Experiment (TOGA–COARE) simulations, *J. Geophys. Res.*, *113*, D19305, doi:10.1029/2008JD009942.

Broecker, W. S., D. McGee, K. D. Adams, H. Cheng, R. L. Edwards, C. G. Oviatt, and J. Quade (2009), A great basin-wide dry episode during the first half of the Mystery Interval?, *Quat. Sci. Rev.*, *28*, 2557–2563, doi:10.1016/j.quascirev.2009.07.007.

Carvalho, L. M. V., C. Jones, and B. Liebmann (2004), The South Atlantic Convergence Zone: Intensity, form, persistence, and relationships with intraseasonal to interannual activity and extreme rainfall, *J. Clim.*, *17*, 88–108.

Chen, T.-C., and S.-P. Weng (1999), Maintenance of austral summertime upper-tropospheric circulation over tropical South America: The Bolivian High–Nordeste Low System, *Atmos. Res.*, *56*, 2081–2100, doi:10.1175/1520-0469(1999)056<2081:MOASUT>2.0.CO;2.

Cheng, H., A. Sinha, X. Wang, F. W. Cruz, and R. L. Edwards (2012), The global paleomonsoon as seen through speleothem records from Asia and the Americas, *Clim. Dyn.*, *39*, 1045–1062, doi:10.1007/s00382-012-1363-7.

Cheng, H., et al. (2013a), Improvements in ^{230}Th dating, ^{230}Th and ^{234}U half-life values, and U–Th isotopic measurements by multi-collector inductively coupled plasma mass spectrometry, *Earth Planet. Sci. Lett.*, *371–371*, 82–91, doi:10.1016/j.epsl.2013.04.006.

Cheng, H., A. Sinha, F. W. Cruz, X. Wang, R. L. Edwards, F. M. d'Horta, C. C. Ribas, M. Vuille, L. D. Stott, and A. S. Auler (2013b), Climate change patterns in Amazonia and biodiversity, *Nat. Commun.*, *4*, 1411, doi:10.1038/ncomms2415.

Chiang, J. C. H., and C. M. Bitz (2005), Influence of high latitude ice cover on the marine Intertropical Convergence Zone, *Clim. Dyn.*, *25*, 477–496, doi:10.1007/s00382-005-0040-5.

Chiessi, C. M., S. Mulitza, J. Pätzold, G. Wefer, and J. A. Marengo (2009), Possible impact of the Atlantic Multidecadal Oscillation on the South American summer monsoon, *Geophys. Res. Lett.*, *36*, L21707, doi:10.1029/2009GL039914.

Cruz, F. W., S. J. Burns, I. Karmann, W. D. Sharp, M. Vuille, A. O. Cardoso, J. A. Ferrari, P. L. Silva Dias, and O. Viana Jr. (2005), Insolation-driven changes in atmospheric circulation over the past 116 ky in subtropical Brazil, *Nature*, *434*, 63–66, doi:10.1038/nature03365.

Cvijanovic, I., and J. C. H. Chiang (2013), Global energy budget changes to high latitude North Atlantic cooling and the tropical ITCZ response, *Clim. Dyn.*, *40*, 1435–1452, doi:10.1007/s00382-012-1482-1.

Dupont, L. M., F. Schlutz, C. Ewah, T. C. Jennerjaahn, A. Paul, and H. Behling (2010), Two-step vegetation response to enhanced precipitation in Northeast Brazil during Heinrich event 1, *Global Change Biol.*, *16*, 1647–1660, doi:10.1111/j.1365-2486.2009.02023.x.

Escobar, J., et al. (2012), A ~43-ka record of paleoenvironmental change in the Central American lowlands inferred from stable isotopes of lacustrine ostracods, *Quat. Sci. Rev.*, *37*, 92–104, doi:10.1016/j.quascirev.2012.01.020.

Fischer, D., J. M. Mogollón, M. Strasser, T. Pape, G. Bohrmann, N. Fekete, V. Spiess, and S. Kasten (2013), Subduction zone earthquake as potential trigger of submarine hydrocarbon seepage, *Nat. Geosci.*, *6*, 647–651, doi:10.1038/ngeo1886.

Fischer, G., et al. (1996), Report and preliminary results of meteor-cruise M34/4, Berichte Fachbereich Geowissenschaften, Universität Bremen, *80*, 1–105.

Gandu, A. W., and P. L. Silva Dias (1998), Impact of tropical heat sources on the South American tropospheric upper circulation and subsidence, *J. Geophys. Res.*, *103*, 6001–6015, doi:10.1029/97JD03114.

Govin, A., U. Holzwarth, D. Helsop, L. F. Keeling, M. Zabel, S. Mulitza, J. A. Collins, and C. Chiessi (2012), Distribution of major elements in Atlantic surface sediments (36 N–49 S): Imprint of terrigenous input and continental weathering, *Geochem. Geophys. Geosyst.*, *13*, Q01013, doi:10.1029/2011GC003785.

Hastenrath, S. (1990), Prediction of Northeast Brazil rainfall anomalies, *J. Clim.*, *3*, 893–904, doi:10.1175/1520-0442(1990)0032.0.CO;2.

Heinrich, H. (1988), Origin and consequences of cyclic ice rafting in the northeast Atlantic Ocean during the past 130,000 years, *Quart. Res.*, *29*(2), 142–152, doi:10.1016/0033-5894(88)90057-9.

Hemming, S. R. (2004), Heinrich events: Massive Late Pleistocene detritus layers of the North Atlantic and their global climate imprint, *Rev. Geophys.*, *42*, RG1005, doi:10.1029/2003RG000128.

Hopmans, E. C., J. W. H. Weijers, E. Schefuß, L. Herfort, J. S. S. Damsté, and S. Schouten (2004), A novel proxy for terrestrial organic matter in sediments based on branched and isoprenoid tetraether lipids, *Earth Planet. Sci. Lett.*, *255*, 107–116, doi:10.1016/S0277-3791(03)00204-X.

Jaeschke, A., C. Rühlemann, H. Arz, G. Heil, and G. Lohmann (2007), Coupling of millennial-scale changes in sea surface temperature and precipitation off northeastern Brazil with high-latitude climate shifts during the last glacial period, *Paleoceanography*, *22*, PA4206, doi:10.1029/2006PA001391.

Marengo, J. A., et al. (2012), Recent developments on the South American monsoon system, *Int. J. Climatol.*, *32*, 1–12, doi:10.1002/joc.2254.

Martrat, B., P. Jimenez-Amat, R. Zahn, and J. O. Grimalt (2014), Similarities and dissimilarities between the last two deglaciations and interglaciations in the North Atlantic region, *Quat. Sci. Rev.*, *99*, 122–134, doi:10.1016/j.quascirev.2014.06.016.

Mosblech, N. A. S., et al. (2012), North Atlantic forcing of Amazonian precipitation during the Last Ice Age, *Nature*, *5*, 817–820, doi:10.1038/NGEO1588.

Pailler, D., and E. Bard (2002), High frequency palaeoceanographic changes during the past 140000 yr recorded by the organic matter in sediments of the Iberian Margin, *Palaeogeogr. Palaeoclimatol. Palaeoecol.*, *181*, 431–452, doi:10.1177/0959683609350391.

Rao, V. B., I. F. A. Cavalcanti, and K. Hada (1996), Annual variation of rainfall over Brazil and water vapor characteristics over South America, *J. Geophys. Res.*, *101*, 26,539–26,551, doi:10.1029/96JD01936.

Rasmussen, S. O., I. K. Seierstad, K. K. Andersen, M. Bigler, D. Dahl-Jensen, and S. J. Johnsen (2006), Synchronization of the NGRIP, GRIP, and GISP2 ice cores across MIS 2 and palaeoclimatic implications, *Quat. Sci. Rev.*, *27*, 18–28, doi:10.1016/j.quascirev.2007.01.016.

Rasmussen, S. O., et al. (2014), stratigraphic framework for abrupt climatic changes during the Last Glacial period based on three synchronized Greenland ice-core records: Refining and extending the INTIMATE event stratigraphy, *Quat. Sci. Rev.*, *106*, 14–28, doi:10.1016/j.quascirev.2014.09.007.

Risi, C., S. Bony, and F. Vimeux (2008), Influence of convective processes on the isotopic composition (δ^{18}O and δD) of precipitation and water vapor in the tropics: 2. Physical interpretation of the amount effect, *J. Geophys. Res.*, *113*, D19306, doi:10.1029/2008JD009943.

Rozanski, K., S. L. Araguás-Araguá, and R. Gonfiantini (1993), Isotopic patterns in modern global precipitation, in *Climate Change in Continental Isotopic Records*, edited by P. K. Swart et al., pp. 1–37, AGU, Washington, D. C.

Sánchez-Goñi, M. F., and S. P. Harrison (2010), Millennial-scale climate variability and vegetation changes during the Last Glacial: Concepts and terminology, *Quat. Sci. Rev.*, *29*, 2823–2827, doi:10.1016/j.quascirev.2009.11.014.

Schouten, S., E. C. Hopmans, and J. S. Sinninghe Damsté (2013), The organic geochemistry of glycerol dialkyl glycerol tetraether lkpids: A review, *Org. Geochem.*, *54*, 19–61, doi:10.1016/jorggeochem.2012.09.006.

Stager, J. C., D. B. Ryves, B. M. Chase, and F. S. R. Pausata (2011), Catastrophic drought in the Afro-Asian monsoon region during Heinrich Event 1, *Science*, *331*, 1299–1302, doi:10.1126/science.1198322.

Thouveny, N., E. Moreno, D. Delanghe, L. Candon, Y. Lancelot, and N. J. Shackleton (2000), Rock magnetic detection of distal ice-rafted debries: Clue for the identification of Heinrich layers on the Portuguese margin, *Earth Planet. Sci. Lett.*, *180*, 61–75, doi:10.1016/S0012-821X(00)00155-2.

Vera, C., et al. (2006), Toward a unified view of the American monsoon systems, *J. Clim.*, *19*, 4977–5000, doi:10.1175/JCLI3896.1.

Vuille, M., and M. Werner (2005), Stable isotopes in precipitation recording South American summer monsoon and ENSO variability: Observations and model results, *Clim. Dyn.*, *25*, 401–413, doi:10.1007/s00382-005-0049-9.

Vuille, M., R. S. Bradley, M. Werner, R. Healy, and F. Keimig (2003), Modeling δ^{18}O in precipitation over the tropical Americas: 1. Interannual variability and climatic controls, *J. Geophys. Res.*, *108*(D6), 4174, doi:10.1029/2001JD002038.

Wang, X., A. S. Auler, R. L. Edwards, H. Cheng, P. S. Cristalli, P. L. Smart, D. A. Richards, and C.-C. Shen (2004), Wet periods in northeastern Brazil over the past 210 kyr linked to distant climate anomalies, *Nature*, *432*, 740–743, doi:10.1038/nature03067.

Wang, Y. J., H. Cheng, R. L. Edwards, Z. S. An, J. Y. Wu, C.-C. Shen, and J. A. Dorale (2001), A high-resolution absolute-dated Late Pleistocene monsoon record from Hulu Cave, China, *Science*, *294*, 2345–2348, doi:10.1126/science.1064618.

Zhang, W., J. Wu, Y. Wang, Y. Wang, H. Cheng, X. Konga, and F. Duan (2014), A detailed East Asian monsoon history surrounding the 'Mystery Interval' derived from three Chinese speleothem records, *Quat. Res.*, *82*, 154–163, doi:10.1016/j.yqres.2014.01.010.